JOURNAL OF MATERIALS SCIENCE **38** (2003) 2639–2646

Relationships between secondary dendrite arm spacing and mechanical properties of Zn-40Al-Cu alloys

M. Ş. TURHAL, T. SAVAŞKAN
Mechanical Engineering Department, Karadeniz Technical University, 61080-Trabzon, Turkey
E-mail: savaskan@ktu.edu.tr

Three ternary monotectoid-based Zn-40Al-(1, 2, 3%) Cu alloys were produced by permanent mould casting at different pouring and mould temperatures. The average cooling rate for each alloy was determined. Structure of the alloys was examined using optical and electron microscopes and their hardness, tensile strength, percentage elongation and impact energy were measured. As a result of these investigations the relationships between structure and mechanical properties of the alloys were determined.

It was observed that the secondary dendrite arm spacing of the alloys decreased with increasing cooling rate and their hardness, tensile strength, percentage elongation and impact energy increased. Correlation of experimental results showed that the hardness, tensile strength, percentage elongation and impact energy of the alloys could be related to their secondary dendrite arm spacing using straight line equations.

1. Introduction

It is known that zinc-based commercial alloys have good mechanical and tribological properties and therefore they have been used in many engineering applications [1–6]. It is also known [7–10] that the mechanical properties of these alloys may be further improved by controlling their microstructure. Cooling rate was found to be one of the effective parameters to control the microstructure of the as-cast alloys [10, 11]. It was observed that as the cooling rate increased the secondary dendrite arm spacing of the alloys decreased. Decreasing the secondary dendrite arm spacing resulted in an increase in tensile strength of the alloys [10, 12]. Skenazi *et al*. [13] found a relationship between tensile strength and secondary dendrite arm spacing of zinc-based commercial alloys. However his work was carried out only on the eutectic and eutectoid-based ZA-8, ZA-12 and ZA-27 commercial alloys produced by sand casting and the relationships between structure and other mechanical properties of these alloys were not included. On the other hand the monotectoid-based Zn—Al alloys have been found to have higher strength and wear resistance than either eutectic or eutectoid-based alloys [11, 14, 15] As a result of this most of the research work on Zn—Al alloys has been concentrated on the monotectoid composition [16–24]. However the relationships between structure and properties of these alloys have not been fully established. It is therefore the purpose of this work to determine the relationships between secondary dendrite arm spacing and mechanical properties of Zn-40Al-Cu alloys produced by permanent mould casting.

2. Experimental procedure

2.1. Production and testing of alloys

High purity zinc (%99.9), electrolytic copper (%99.9) and commercially pure aluminium were used to produce the alloys. The alloys were melted in an electrical resistance type furnace using a silicon carbide crucible and poured from different melting temperatures ranging from 600°C to 700°C into a permanent mould. The mould was kept at different temperatures between 0°C and 300°C. The mould was produced from mild steel and the shape and size of it is given in Fig. 1. The cooling curves of the alloys were plotted during casting using chromel-alumel type thermocouples placed at fixed distances along the sideline of the ingots and an analogue-digital converter in a computer. The average cooling rates for the ingots of each alloy were determined by taking the slope of the cooling curves between liquidus and solidus temperatures. The liquidus temperature of the alloys was determined from the binary Zn—Al and the ternary Zn—Al—Cu phase diagrams as 525°C, and their solidus temperature was taken as 375°C according to the literature [25–28].

Chemical compositions of the alloys were determined by atomic absorption analysis. Samples for structural examination were prepared using standard metallographic techniques and etched in 10% Nital. The samples were then examined using both a light microscope and a scanning electron microscope (SEM). Secondary dendrite arm spacing of the alloys was measured using line intercept method and at least thirty readings were taken to determine the average value of

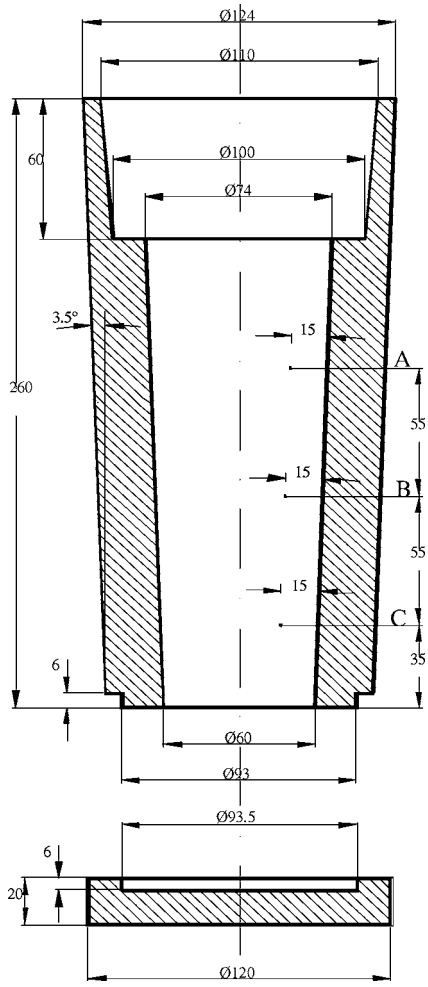

Figure 1 Shape and size of the mould.

it. The percentage porosity of the alloys was determined using an equation given in the literature [9]. This equation is given below.

$$\text{Percentage porosity } (\%) = (\rho_f - \rho_m)/\rho_f \times 100 \quad (1)$$

where ρ_f is the full density and ρ_m is the measured density of the alloys.

Tensile tests were carried out on round specimens with a diameter of 10 mm and a gauge length of 50 mm using a tensile test machine at a strain rate of 0.006 s^{-1}. Brinell hardness of the alloys was measured using a load of 31.25 kg and a 2.5 mm diameter ball as an indenter. The hardness of the alloys was determined by taking the average of five hardness readings. Impact tests were carried out on these alloys using unnotched Charpy specimens which have the dimensions of 10 × 10 × 55 mm. The impact energy of the alloys was determined by taking the average of two readings.

3. Results

3.1. Chemical compositions, cooling rates and secondary dendrite arm spacing

Chemical compositions of the alloys are given in Table I. Typical examples of the cooling curves obtained from three different points of the Zn-40Al-2Cu casting are given in Figs 2 and 3. In these figures Tp and Tm show the pouring and the mould temperatures respectively.

TABLE I Chemical composition of the alloys

	Chemical composition (wt%)		
Alloy	Zn	Al	Cu
Zn-40Al-1Cu	59.2	39.7	1.1
Zn-40Al-2Cu	57.9	40.0	2.1
Zn-40Al-3Cu	58.0	39.0	3.0

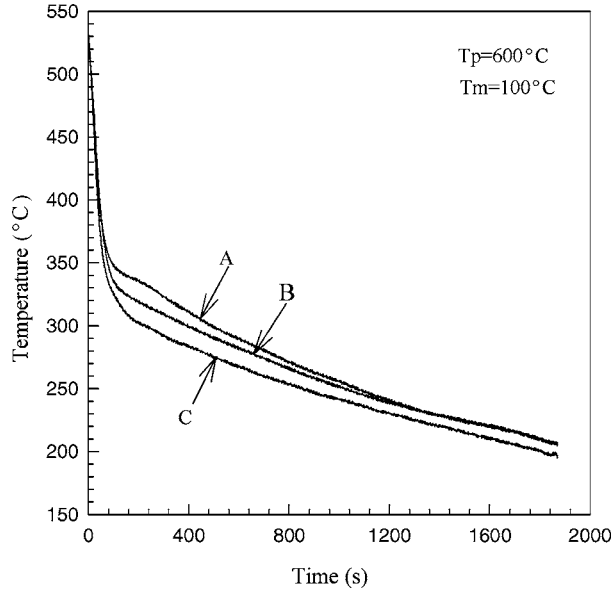

Figure 2 Cooling curves for three points of Zn-40Al-1Cu alloy produced by pouring from 600°C into a mould at 100°C.

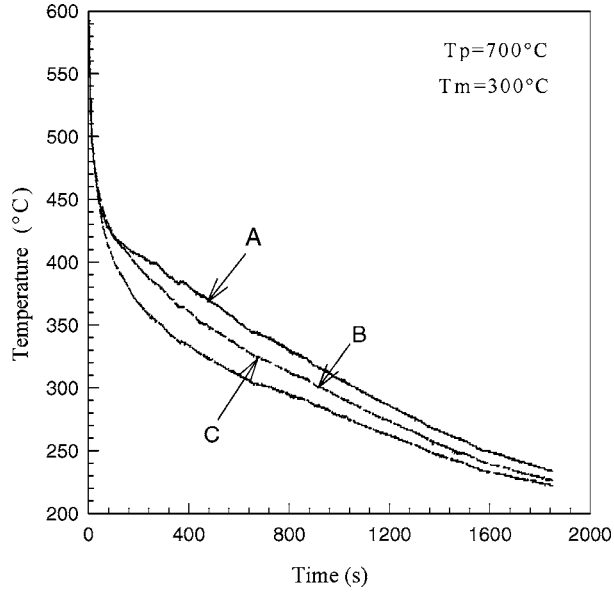

Figure 3 Cooling curves for three points of Zn-40Al-2Cu alloy produced by pouring from 700°C into a mould at 300°C.

The microstructure of the alloys produced at different cooling rates consisted of aluminium-rich α dendrites, zinc-rich η and copper-rich T′ phases in the interdendritic regions. This can be seen on the micrographs obtained from Zn-40Al-1Cu, Zn-40Al-2Cu and Zn-40Al-3Cu alloys, Figs 4a, b, 5a, b, 6a

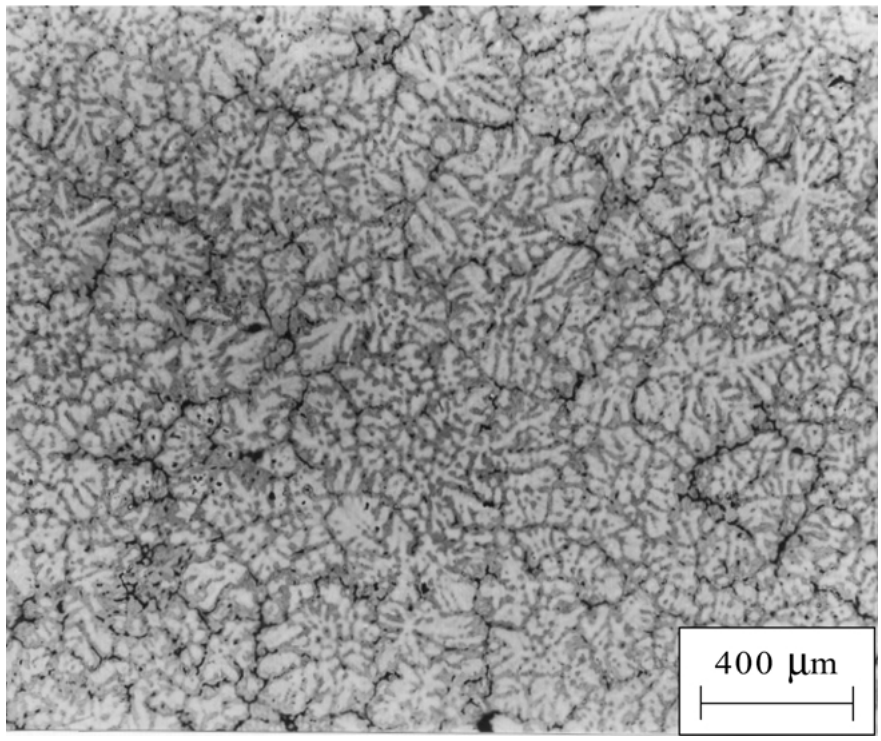

(a)

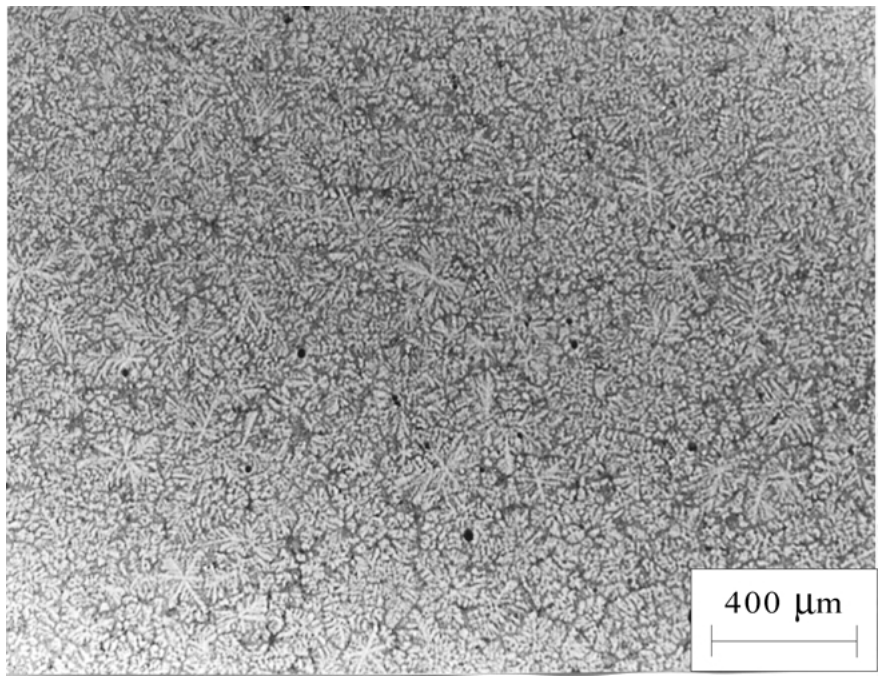

(b)

Figure 4 (a) Microstructure of Zn-40Al-1Cu alloy produced at a cooling rate of 1.23°C/s. (b) Microstructure of Zn-40Al-1Cu alloy produced at a cooling rate of 4.56°C/s.

and b respectively. These micrographs show that as the cooling rate increases the primary dendrite size of the alloys decreases. The secondary dendrite arm spacing of the alloys was also decreased with increasing cooling rate. The cooling rates and the secondary dendrite arm spacing of the alloys produced are given in Table II. The effect of cooling rate on the dendrite arm spacing is shown in Fig. 7. It can be seen from this figure that as the cooling rate increases the secondary dendrite arm spacing of the alloys decreases.

3.2. Relationships between secondary dendrite arm spacing and mechanical properties of the alloys

The secondary dendrite arm spacing and the mechanical test results obtained from the alloys are given in Table III. The curves of the hardness, tensile strength, percentage elongation and impact energy of the alloys versus secondary dendrite arm spacing are shown in Figs 8–11 respectively. It can be seen from these curves that the hardness, tensile strength, percentage elongation and impact energy of the alloys increase

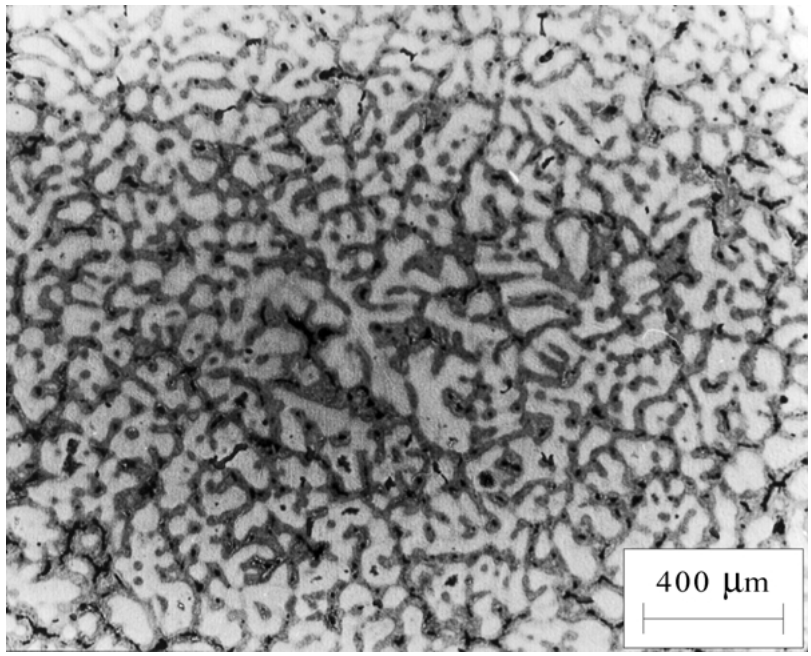

(a)

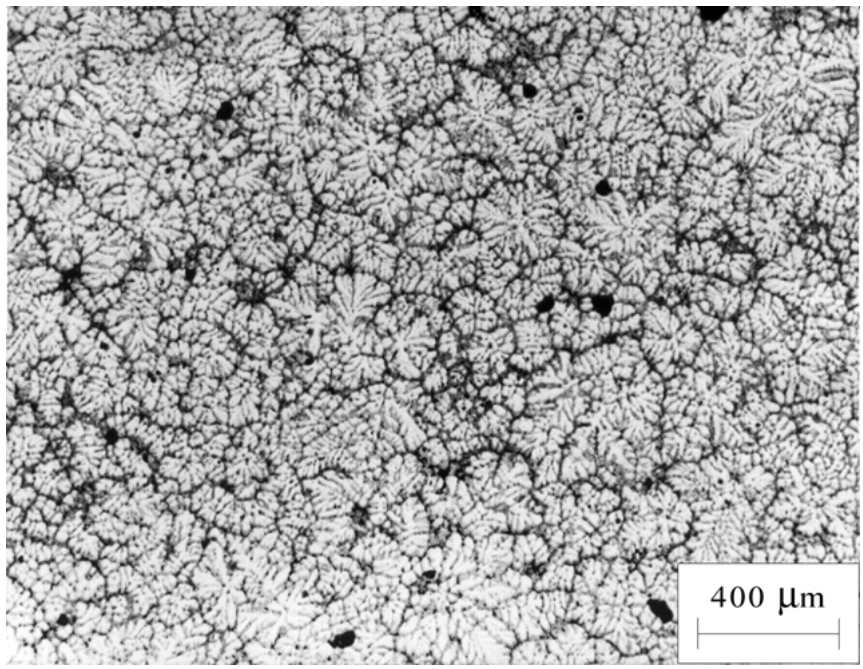

(b)

Figure 5 (a) Microstructure of Zn-40Al-2Cu alloy produced at a cooling rate of 0.33°C/s. (b) Microstructure of Zn-40Al-2Cu alloy produced at a cooling rate of 4.46°C/s.

with decreasing secondary dendrite arm spacing. It was found that the hardness (H), tensile strength (σ_{TS}), percentage elongation ($\varepsilon\%$) and impact energy (E) of the alloys can be related to their secondary dendrite arm spacing (d) using straight line equations given below.

$$H = Ad + B \tag{2}$$

$$\sigma_{TS} = Ad + B \tag{3}$$

$$\varepsilon(\%) = Ad + B \tag{4}$$

$$E = Ad + B \tag{5}$$

where A and B are constants. These constants and correlation coefficients for the alloys are given in Tables IV–VII respectively.

4. Discussion

In this work, it was found that the secondary dendrite arm spacing of the alloys decreased with increasing cooling rate. As the cooling rate decreases there is enough time for small dendrite arms to melt and disappear [29]. This occurs as a result of their high surface area to volume ratio that increases their total energy per unit volume. As the small dendrite arms disappear the

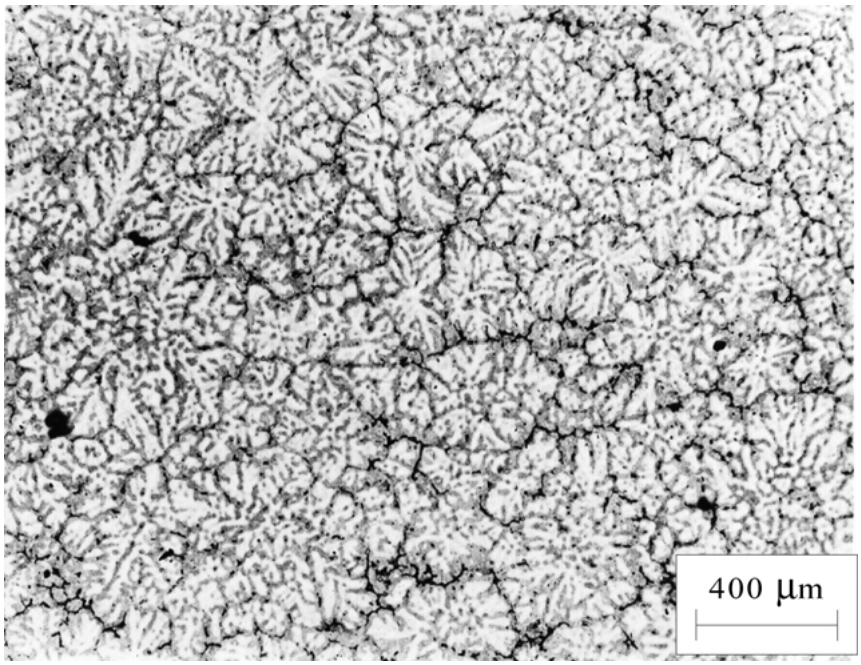

(a)

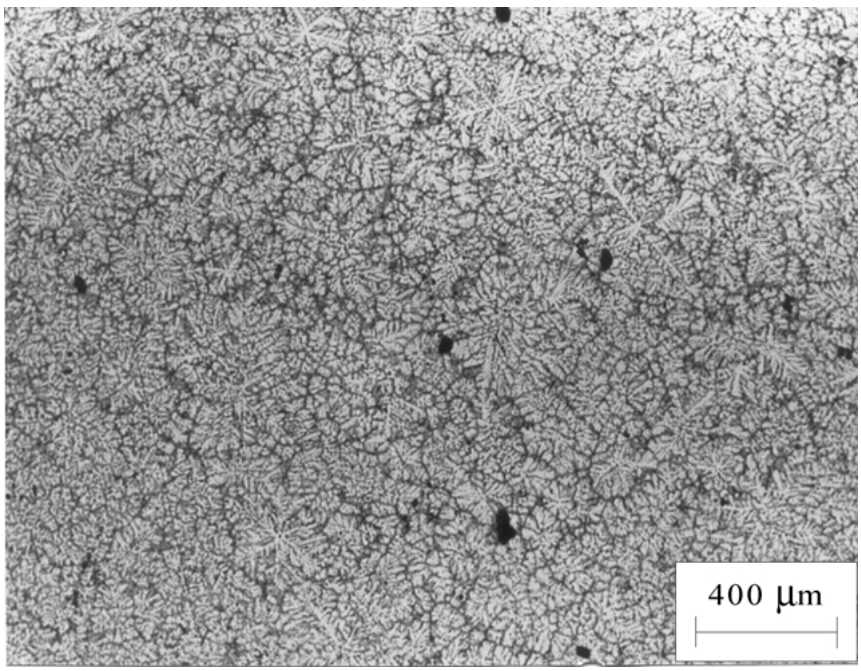

(b)

Figure 6 (a) Microstructure of Zn-40Al-3Cu alloy produced at a cooling rate of 1.15°C/s. (b) Microstructure of Zn-40Al-3Cu alloy produced at a cooling rate of 4.51°C/s.

secondary dendrite arm spacing of the alloys increases [30].

It was also found that the hardness, tensile strength, percentage elongation and impact energy of the alloys increased with decreasing secondary dendrite arm spacing, Figs 8–11. This observation may be explained in terms of microstructure and soundness of the alloys. It was observed that percentage porosity of the alloys decreased with decreasing secondary dendrite arm spacing, Fig. 12. This means that as the secondary dendrite arm spacing decreased the alloys became sounder. Hence as the soundness of the alloys increased their hardness, strength and elongation increased.

It was also found that when the copper content exceeded 2%, tensile strength of these alloys decreased. This may be related to the microstructure of the copper containing alloys. It is known [31] that when the copper content of the Zn–Al–Cu alloys exceeds 2% copper-rich intermetallic T′ and θ phases form in the interdendritic regions. Formation of copper-rich intermetallic phases decreases the copper content of aluminium and zinc rich dendrites and hence reduces the effect of the solid solution strengthening.

Comparison of the relationships obtained between the mechanical properties and the secondary dendrite arm spacing showed that the impact energy and

TABLE II Secondary dendrite arm spacing (d) of the alloys obtained at different cooling rates (R)

Alloy	R (°C/s)	d (μm)
Zn-40Al-1Cu	4.56	21
	2.89	27
	2.28	37
	1.23	46
Zn-40Al-2Cu	4.46	22
	3.15	30
	2.64	37
	2.32	39
	0.91	49
	0.33	54
Zn-40Al-3Cu	4.51	20
	3.35	26
	2.46	34
	1.15	42

TABLE III Hardness (H), tensile strength (σ_{TS}), percentage elongation (ε%) and impact energy (E) of the alloys corresponding to different secondary dendrite arm spacing (d)

Alloy	d (μm)	H (BHN)	σ_{TS} (MPa)	ε(%)	E (J)
Zn-40Al-1Cu	21	116	371	9	45
	27	114	366	8	40
	37	111	361	7	34
	46	108	353	6	31
Zn-40Al-2Cu	22	121	390	9	40
	30	119	384	8	34
	37	116	380	8	30
	39	116	377	7	29
	49	112	373	6	23
	54	111	368	5	19
Zn-40Al-3Cu	20	125	389	5	35
	26	121	383	4	31
	34	119	375	3	26
	42	117	370	3	17

percentage elongation of the alloys are more sensitive to the change in the secondary dendrite arm spacing compared to hardness and tensile strength, Tables IV–VII and Figs 8–11. This observation may be explained

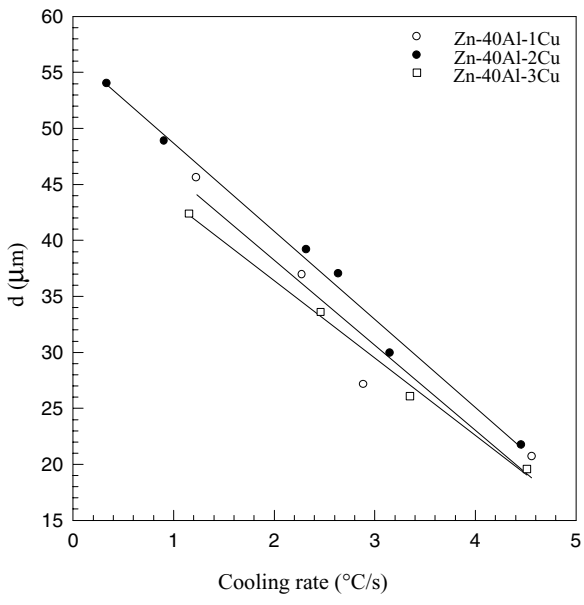

Figure 7 Curves showing the effect of cooling rate on the secondary dendrite arm spacing (d) of the alloys.

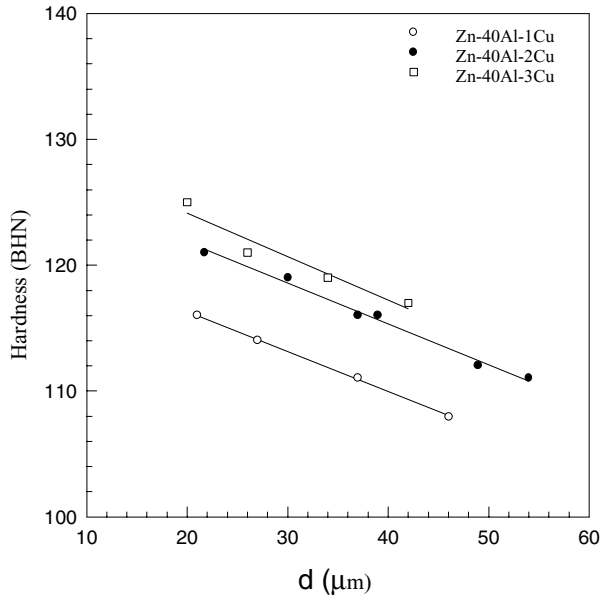

Figure 8 Curves showing the effect of secondary dendrite arm spacing (d) on the hardness of the alloys.

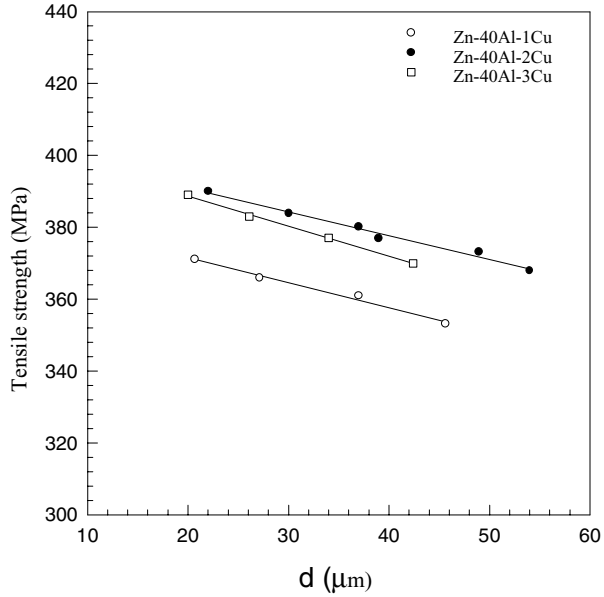

Figure 9 Curves showing the effect of secondary dendrite arm spacing (d) on the tensile strength of the alloys.

in terms of porosity in the alloys. It is known that as the secondary dendrite arm spacing decreases the number of pores in these alloys decreases [9, 10]. It is also known that the hardness and tensile strength of the alloys are not as sensitive as their impact energy and percentage elongation to the change in the percentage porosity [9]. This may be related to the measuring techniques of these parameters. For example surface porosity is expected to be effective on the measured hardness of the alloys compared to internal porosity; however both surface and internal porosity may affect impact energy and elongation. On the other hand porosity is more effective during necking of the alloys, which takes place after the maximum tensile stress is reached. Furthermore, necking may not occur in the alloys containing high percentage porosity and the test pieces may

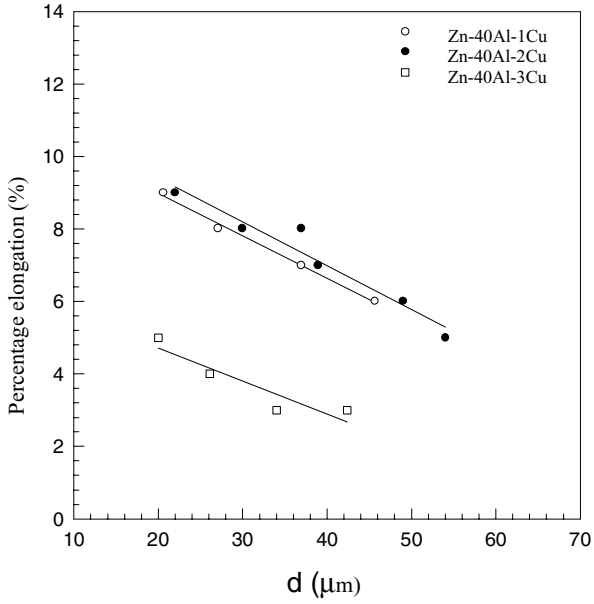

Figure 10 Curves showing the effect of secondary dendrite arm spacing (d) on the percentage elongation of the alloys.

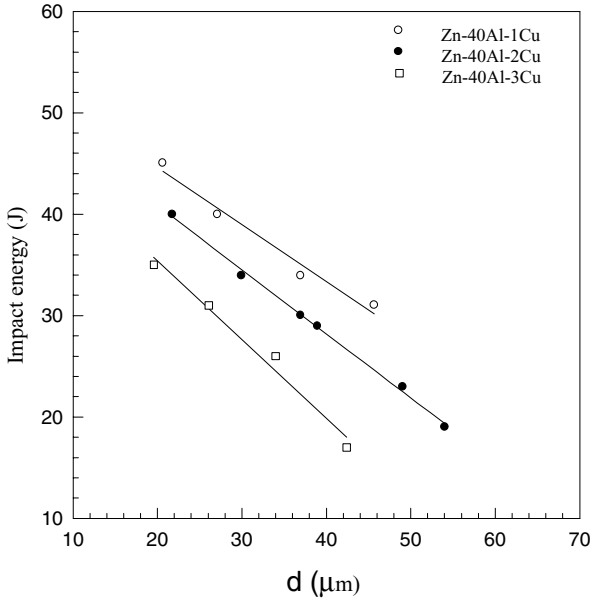

Figure 11 Curves showing the effect of secondary dendrite arm spacing (d) on the impact energy of the alloys.

fracture when or before the maximum tensile stress is reached. This is probably why the tensile strength of the alloys is not as sensitive as their elongation to porosity and hence to the change in the secondary dendrite arm spacing. On the other hand pores may act as notches during impact loading and greatly reduce the impact

TABLE IV Values of A and B constants and correlation coefficient (k) for Equation (2), which shows the relationship between hardness (H) and secondary dendrite arm spacing (d) of the alloys

Alloy	A	B	k
Zn-40Al-1Cu	−0.32	123	0.99
Zn-40Al-2Cu	−0.32	128	0.99
Zn-40Al-3Cu	−0.35	131	0.97

TABLE V Values of A and B constants and correlation coefficient (k) for Equation (3), which shows the relationship between tensile strength (σ_{TS}) and secondary dendrite arm spacing (d) of the alloys

Alloy	A	B	k
Zn-40Al-1Cu	−0.69	385	0.99
Zn-40Al-2Cu	−0.66	404	0.99
Zn-40Al-3Cu	−0.84	405	0.99

TABLE VI Constants (A and B) and correlation coefficient (k) for Equation (4) which shows the relationship between percentage elongation ($\varepsilon\%$) and secondary dendrite arm spacing (d) of the alloys

Alloy	A	B	k
Zn-40Al-1Cu	−0.12	11	0.99
Zn-40Al-2Cu	−0.12	12	0.98
Zn-40Al-3Cu	−0.09	7	0.92

TABLE VII Constants (A and B) and correlation coefficient (k) for Equation (5) which shows the relationship between the impact energy (E) and secondary dendrite arm spacing (d) of the alloys

Alloy	A	B	k
Zn-40Al-1Cu	−0.56	56	0.99
Zn-40Al-2Cu	−0.63	54	0.99
Zn-40Al-3Cu	−0.78	51	0.99

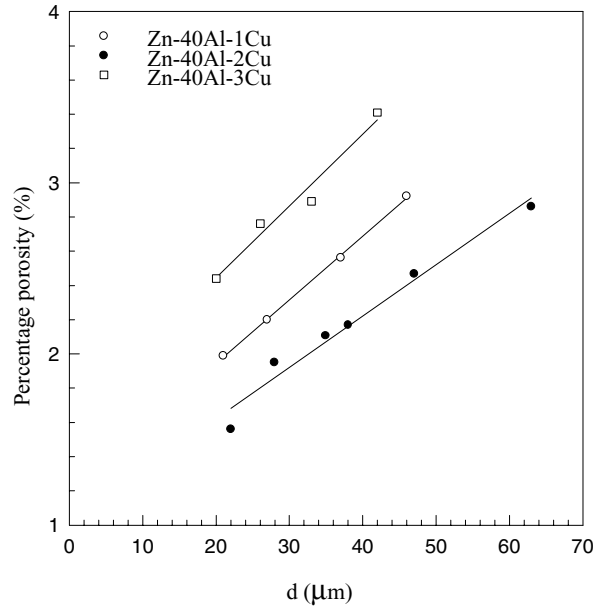

Figure 12 Curves showing effect of secondary dendrite arm spacing (d) on the percentage porosity of the alloys.

energy of the alloys. This is because notches are more effective on the mechanical behaviour of alloys under dynamic loading than they are under static loading [32, 33].

5. Conclusions

1. Secondary dendrite arm spacing of Zn-40Al-Cu alloys decreases with increasing cooling rate during solidification. As the secondary dendrite arm spacing

decreases the hardness, tensile strength, percentage elongation and impact energy of these alloys increase.

2. The hardness, tensile strength, percentage elongation and impact energy of Zn-40Al-Cu alloys in the as-cast condition can be related to their secondary dendrite arm spacing using straight line equations.

3. Secondary dendrite arm spacing strongly affects the impact energy and elongation of Zn-40Al-Cu alloys but has less effect on their hardness and tensile strength.

Acknowledgements

This work was supported by the Research Fund of Karadeniz Technical University. The authors would like to thank all the technicians in the Materials Division and Machine Shop of the Mechanical Engineering Department of above university for their help.

References

1. E. GERVAIS and C. A. LOONG, in "11th International Pressure Die Casting Conference," (Lyon, France, 19–22 June 1984) p. 1.
2. D. APELIAN, M. PALIWAL and D. C. HERRSCAFT, *Journal of Metals* (1981) 12.
3. E. GERVAIS, *CIM Bulletin* (1987) 67.
4. S. MURPHY and T. SAVAŞKAN, *Wear* **98** (1984) 151.
5. T. SAVAŞKAN and S. MURPHY, *ibid.* **116** (1987) 211.
6. P. P. LEE, T. SAVAŞKAN and E. E. LAUFER, *ibid.* **117** (1987) 79.
7. W. MIHAICHUK, *Modern Casting* (1981) 39.
8. M. A. SAVAŞ and S. ALTINTAŞ, *J. Mater. Sci.* **28** (1993) 1775.
9. F. ASHRAFIZADEH, J. M. YOUNG and V. KONDIC, *Materials Science and Technology* **3** (1987) 665.
10. R. J. BARNHURST, E. GERVAIS and F. D. BAYLES, *AFS Transactions* **91** (1983) 569.
11. T. SAVAŞKAN, M. Ş. TURHAL and S. MURPHY, *Materials Science and Technology* **19** (2003) 67.
12. S. LING and M. P. ANDERSON, *JOM* (1992) 30.
13. A. F. SKENAZI, J. PELERIN, D. COUTSOURADIS, B. MAGNUS and M. MEEUS, *Metall* **9** (1983) 898.
14. T. SAVAŞKAN, M. AYDIN and H. A. ODABAŞIOĞLU, *Materials Science and Technology* **17** (2001) 681.
15. G. PÜRÇEK, T. SAVAŞKAN, T. KÜÇÜKÖMEROĞLU and S. MURPHY, *Wear* **252** (2002) 894.
16. S. MURPHY, T. SAVAŞKAN and J. K. WHEELDON, Casting and Foundry Technology, International Congress on Metals Engineering, 15–16 September 1981, p. 7.1.
17. T. SAVAŞKAN and S. MURPHY, *Materials Science and Technology* **6** (1990) 695.
18. M. S. SAKR, A. E. E. ABDEL-ELRAAHEIM and A. A. EL-DALLY, *Phys. Stat. Solid (A)* **94** (1986) 561.
19. G. HAORAN, T. XIANFA, C. HONGWEI, L. CHENGDONG and Z. PENG, *Materials Science and Engineering* **A 316** (2001) 109.
20. B. K. PRASAD, *Materials Transactions JIM* **8** (1997) 701.
21. B. K. PRASAD, *Materials Characterization* **44** (2000) 301.
22. O. M. MODI, R. P. YADAV, B. K. PRASAD, A. K. JHA, S. DAS and A. H. YEGNESWARAN, *Z. Metallkd.* **90** (1999) 439.
23. P. P. LEE, T. SAVAŞKAN and E. LAUFER, *Wear* **117** (1987) 79.
24. B. K. PRASAD, A. K. PATWARDHAN and A. H. YEGNESWARAN, *Z. Metallkunde* **88** (1997) 333.
25. A. A. PRENSYAKOV, Y. A. GORBAN and V. V. CHERVYAKOVA, *Russian Journal of Physical Chemistry* **6** (1961) 632.
26. W. KÖSTER, *Zeitschrift für Metallkunde* **33** (1941) 289.
27. E. GERVAIS, R. J. BARNHURST and C. A. LOONG, *J. of Metals* (1985) 43.
28. R. J. BARNHURST, "Gravity Casting Manuel for Zinc-Aluminium Alloys," (Noranda Sales Corporation Ltd., Toronto, 1989) p. 3.
29. J. CAMPBELL, in "Castings," (Reed Educational and Professional Publishing Ltd., Great Britain, 1999) p. 146 and 265.
30. T. Z. KATTAMIS, J. COUGHLIN and M. C. FLEMINGS, *Trans. Met. Soc. AIME* **239** (1967) 1504.
31. S. MURPHY, *Z. Metallkunde* **71** (1980) 96.
32. F. ERDOĞAN, *International Journal of Solids and Structures* **37** (2000) 171.
33. B. R. LAWN and T. R. WILSHAW, in "Fracture of Brittle Solids" (Cambridge University Press, Cambridge, 1975) p. 91.

Received 2 August 2002
and accepted 3 April 2003